

# Vegetation Change Detection Analysis Using Multi-sensor Hyperspectral Imagery

Wahyu Ananta Nugraha<sup>1</sup>, Pramaditya Wicaksono<sup>2</sup>, Sanjiwana Arjasakusuma<sup>2</sup>

<sup>1</sup> Master in Remote Sensing, Universitas Gadjah Mada, Yogyakarta, Indonesia

<sup>2</sup> Department of Geographic Information Science, Universitas Gadjah Mada, Yogyakarta, Indonesia

\*Correspondent Email: [wahyu.ananta.n@mail.ugm.ac.id](mailto:wahyu.ananta.n@mail.ugm.ac.id)

Received 2024-01-23 | Revision 2024-07-25 | Accepted 2024-07-31

Geography Study Program, Lambung Mangkurat University

**Abstract:** Vegetation is a fundamental component of ecosystems that maintains carbon levels, hydrological cycles, mitigating greenhouse gases, and ensures climate stability. In recent years, the impacts of global climate change have led to changes in vegetation cover at various levels. Efforts to monitor changes in vegetation are important and beneficial for various fields such as forest monitoring, agriculture, and plantations, among others. The main objective of this research is to detect changes both increase and decrease in vegetation using multi-sensor hyperspectral imagery. The hyperspectral images used in this study are Hyperion 2014 and PRISMA 2021. The method involves creating different levels of spectral resolution simulations from hyperspectral images to detect vegetation changes. Meanwhile, the vegetation change Clustering method employs unsupervised (k-means) techniques. The cluster results can indicate vegetation changes such as vegetation degradation, vegetation, or no change, though they currently have low accuracy. The highest accuracy is by Simulated RapidEye image simulations, is 33.5%. The low accuracy results attributed insufficient preprocessing, particularly in topographic correction. Additionally, this research indicates that the spectral resolution levels do not have a significant impact on vegetation change detection, as the differences in change classes at each level are very small.

**Keywords:** : *Change Detection, Hyperspectral, CVA, k-means*

## INTRODUCTION

Vegetation is a fundamental component of terrestrial ecosystems that continues to experience changes both naturally and due to the influence of anthropogenic activities. Vegetation also has a role in cycling land, exchanging energy, and cycling biogeochemistry at the surface earth. In recent years, vegetation changes have occurred in varying degrees and ways influenced by global climate and human intervention (Sun et al., 2022). Specifically, deforestation and the degradation of forests become a main threat to the ecosystem especially tropical forests with an average

rate of forest loss of 3.7 million ha per year in the 2010s (González-González et al., 2021). Therefore, further study of vegetation changes is very important.

Remote sensing is the science and art of obtaining information about an object, area, or phenomenon without direct contact, through analysis of the data obtained from certain devices (Lillesand et al., 2015a). This is possible because different objects reflect, absorb, and emit electromagnetic radiation uniquely depending on their molecular composition and texture (Ghamisi, Yokoya, et al., 2017). In the last two decades, hyperspectral remote sensing technology has

advanced rapidly, enabling highly detailed spectral observations to identify materials with a higher degree of accuracy than multispectral imagery (Khan et al., 2018). However, hyperspectral data classification is a significant challenge due to the imbalance between the number of available training samples, and the high dimensionality of the data (Ghamisi, Plaza, et al., 2017).

Hyperspectral imagery shows different radiation intensities corresponding to different material properties, where the characteristics possibly detect and distinguish subtle differences between land cover classes (Chunhui et al., 2018). By the more spectral information, hyperspectral imagery has more used in various applications, such as target detection, change detection, and classification (Fang et al., 2018). In 2000, NASA launched a hyperspectral sensor namely Hyperion EO-1 with 242 spectral bands, a resolution spatial of 30 meters, and a spectral resolution of 10 nanometres. This sensor operated to meet the wide global demand in various fields such as agriculture, forestry, and geology (Tripathi et al., 2019).

Recently, a new hyperspectral sensor called Precursor Iperspettrale della Missione Applicativa (PRISMA) was launched, which is expected to improve dataset quality and temporal resolution. This makes hyperspectral Change Detection (HSCD) an interesting topic among researchers (Hasanlau & Seydi, 2018). In remote sensing, change detection is one of the main applications enabled by satellites and the key technique for detecting changes in land use and land cover. (Chughtai et al., 2021). One method that can be used to detect land changes is Change Vector Analysis (CVA). CVA functions automatically,

sophisticatedly, and efficiently to categorize changes by combining magnitude and direction angle (Kuzera et al., n.d.).

Several studies have been conducted on change detection using unsupervised multi-temporal imagery. Based on the unit of analysis, change detection can categorized as a pixels-based method and object-based method, a specific procedure, and its optimal target objective (Zheng et al., 2021). Generate difference maps by comparing corresponding pixels in the used bitemporal image, and then change maps are generated by threshold segmentation or other strategies (Ghosh et al., 2009). One of the widely used pixel-based change detection methods is the k-means method which is included in unsupervised classification as carried out by (Celik, 2009; Liu et al., 2012).

Based on those theories, monitoring vegetation changes becomes very important. This study aims to detect vegetation changes, both increases and decreases, using multi-sensor hyperspectral imagery.

## LITERATURE REVIEWS

### 1. CVA

The CVA method is applied to both image data according to their spectral levels to compress the representation of changes into change variables, namely change magnitude ( $\rho$ ) and direction angle ( $\alpha$ ). Magnitude shows the amount of change while direction provides information about the type of change that has occurred. Based on this, CVA can provide accurate information about the changes that have occurred, but this method has difficulty in determining the threshold between change and no change (Mishra *et al.*, 2017). This is because the change vector contains dynamic information that does not indicate the

absolute position in spectral space at two different dates (Johnson & Kasischke, 1998). To overcome this problem, two classification methods are applied where unsupervised works by grouping. The magnitude and angle direction formulas refer to Liu's research (2015) as follows.

$$\rho = \sqrt{\sum_{b=1}^B (X_D^b)^2} \quad (1)$$

$$\alpha = \arccos \left[ \frac{1}{\sqrt{B}} \left( \sum_{b=1}^B \frac{X_D^b}{\sqrt{\sum_{b=1}^B (X_D^b)^2}} \right) \right] \quad (2)$$

## 2. K-means

The unsupervised k-means method was chosen because it is capable of processing high dimensional and there is no bias confirmation from the operator (Abbassi et al., 2021). The k-means algorithm is a straightforward iterative approach to divide a given data set into a specified number of clusters (k) as per the user's choice (Wu, 2012). K-means repeated data grouping based on similarities in the same cluster and dissimilarities between different clusters (Sinaga & Yang, 2020).

## RESEARCH METHODS

This research is broadly divided into three main stages, namely preprocessing, processing, and validation. Each stage applies its method, and to make it easier to understand, you can see the flowchart in Figure 2. A more complete description of the data and methods used can be seen in the following sub-chapter.

### 1. Research location and image data

This research was conducted in part of the Mount Merapi National Park area. The

research area is shown more clearly in Figure 1. Hyperspectral data in this study used 2 different sensors, namely Hyperion and PRISMA. Hyperion data used level T1 with an acquisition time of 07/30/2014, while PRISMA data used level L2D with an acquisition time of 04/21/2021. The characteristics of both sensors can be seen in full in Table 1.

## 2. Preprocessing

The utilization of multi-temporal and multi-sensor hyperspectral imagery for change detection requires a preprocessing procedure. Multi-temporal and multi-sensor data cause significant differences in image data, namely different geolocations, differences in radiometry (Lu et al., 2004), differences in atmospheric effects (Lu et al., 2014), vegetation phenology (Jensen, 2013; Lillesand et al., 2015), and differences of recording corner. Therefore, this research applied various preprocessing methods namely Geometric Correction using the 1st Order Polynomial transformation method, Atmospheric Correction using the FLAASH method (Visual Information Solutions, 1988), spectral smoothing using the Savitzky Golay method, Spectral Resampling, Radiometric Normalization using Pseudo Invariant Feature (PIF) and Topographic Correction using the C method (Leutner et al., 2019).

Not all of the preprocessing stages are applied to both image data, some are only applied to one image data. Geometric Correction is applied only to PRISMA image data with Hyperion image data as a reference. Atmospheric correction is applied only to Hyperion image data because PRISMA data uses L2D level. Spectral Resampling is applied to PRISMA image data to match its spectral range with

Hyperion image data. Radiometric Normalization is applied to a Hyperion image to minimize radiometric differences from both image data caused by differences in sensors and recording time.

The stages of spectral compilation with different levels using the Spectral Resampling method run in RStudio with the help of the “hsdar” package (Lehnert et al., 2018). The original hyperspectral data with 115 bands was then converted into 2 types of spectral data levels, namely Sentinel 2 equivalent (13 bands) and Rapid Eye equivalent (5 bands). The process of compiling data with different spectra levels requires data center wavelength and FWHM of the target image data.

The wavelength and FWHM data center also use the references provided in the package. After the process, the image level data and the combination of the three will be obtained. The image level dataset in question is the hyperspectral level (HS), sentinel 2A level (S2), Rapid Eye level (RE), sentinel 2A hyperspectral combination level (HSS2), Rapid Eye hyperspectral combination (HSRE), sentinel 2A Rapid Eye combination (S2RE) and sentinel 2A Rapid Eye hyperspectral combination (HSS2RE)

### 3. Processing

Then, data is processed using the image difference method using the CVA method to produce magnitude and angle direction. Then enter the cluster process. The clustering process in this study was carried out using the "cluster" package with a centroid k of 4 and a default iteration of 1000 times. The cluster process produces data that has been clustered but does not yet have class attributes. Then, each class is visually labeled with the help of high-resolution time series images from Maxar Technology.

### 4. Validity

The mapping results obtained from the change detection analysis using the proposed method need to be tested for accuracy to determine the accuracy of the change mapping and to determine the differences in the capabilities of each spectral level applied. The most common criteria used in assessing the Change Detection method are the receiver operating characteristic (ROC) curve, Overall Accuracy (OA), Kappa Coefficient, and others (Seydi & Hasanlou, 2017).

In this study, the mapping results from each method will be tested using the Confusion Matrix method and OA, Producer Accuracy and User Accuracy are calculated using validation data from visual interpretation of high-resolution Maxar Technology imagery time series. The validation sample data used is 200 plots with a size of 60m<sup>2</sup>.

**Figure 1** Research Area

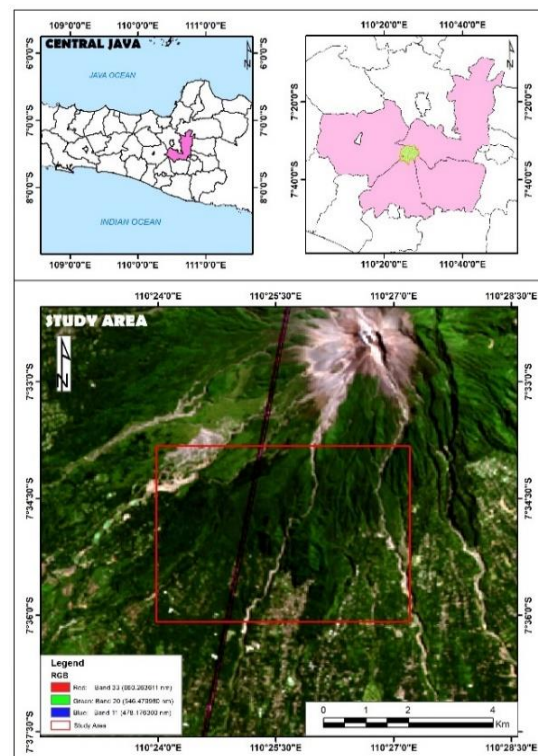


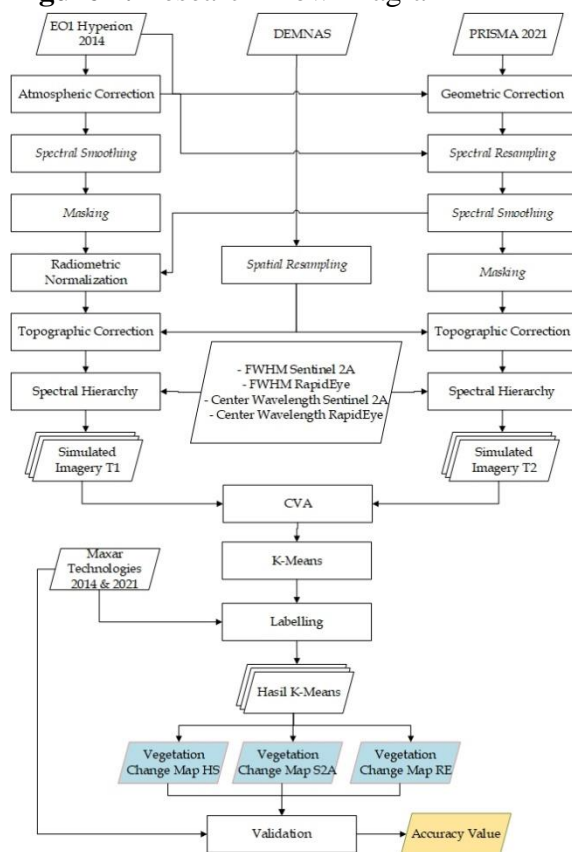
**Table 1.** Image Specifications

Parameter	EO-1 Hyperion	PRISM
Acquisition Date	07-30-2014 [01:36:34]	04-21-2021 [03:05:41]
Spectral Range	0.4-2.39 microns	0.4-2.5 microns
Spatial Resolution	30m	30m
Swath Width	7.5km	30km
Number of Channels	242	231
Temporal Resolution		29 days
Source	USGS NASA EO-1	Italian Space Agency

Source: Cavalli (2023)

database for compiling Sentinel 2A simulation images, Rapid Eye simulation images, and their combinations. The results of the Sentinel 2A image simulation only have 9 spectral bands with the loss of the coastal aerosol band (443 nm), NIR band - vegetation red edge (865 nm), water vapor band (945 nm), and SWIR band - Cirrus (1375 nm). This occurs due to the influence of the application of bad band selection which eliminates spectral bands in the hyperspectral imagery which is the database for image simulation. The entire dataset can be seen in Table 2.

**Figure 2.** Research Flow Diagram



## 2. Results of CVAK-means Method Classification

Magnitude and angle direction results from the image difference process with the CVA method then grouped become four classes using k-means method. The grouping basis uses magnitude data and angle data from each image spectral level and also their combination. Based on this, four classes of changes were produced at each image spectral level in the mapping of vegetation changes in the TNGM Area in 2014 - 2021. The distribution pattern of each group of changes resulting from the k-means method can be seen in Figure 3.

Based on the k-means cluster results, it was found that the level of Sentinel 2A simulation imagery was able to detect the highest "no change" or unchanged class, which was 48.08% with an area of 1224.07 ha. The degradation class was able to be detected the highest at the Rapid Eye simulation imagery level with 27.58% or 702.19 ha. The devegetation class was able to be detected the highest in the combination of hyperspectral imagery with Rapid Eye simulation imagery, which was 19.75% or

## RESULTS AND DISCUSSION

### 1. Datasets

In this study, the dataset uses hyperspectral image data from Hyperion imagery and PRISMA imagery as the

502.91 ha, while the vegetation class was able to be detected the highest at the hyperspectral level with Sentinel 2A simulation imagery with a size of 28.64% or 729.25 ha. The complete results of the class area and percentage can be seen in Table 2.

Based on accuracy test calculations from classification, the k-means have an average of 32%. Application combination image has also been done, but it does not increase the accuracy level of the classification. The highest accuracy value is achieved by the Rapid Eye simulation image level of 33.5%.

The lowest accuracy value of 31% is owned by the combination image level of hyperspectral with Sentinel 2A simulation imagery and a combination of hyperspectral imagery, Sentinel 2A simulation imagery, and RapidEye simulation imagery.

The accuracy results of the k-means classification at all image levels can be seen in Table 3. The spatial distribution of vegetation changes in TNGM in 2014–2021 generally has different patterns at each image level. Differences in change patterns can occur because each image level has a different number of spectral channels, resulting in different sensitivity to recording electromagnetic wave reflections. The composition of the existing spectral channels also affects the cluster results in addition to the quality of the existing data.

While k-means performs classification based on image data with the threshold used

to adjust to the distance at the specified centroid k.

Based on this, the results of the k-means method are highly dependent on the quality of the input data. The low accuracy of k-means results is influenced by the low quality of the input data and can be interpreted as meaning that the preprocessing process was unsuccessful.

This difference in recording angle causes differences in the spectral reflectance received on the sensor, especially on vegetation objects. Vegetation itself is a True Lambertian Surface because it reflects the energy obtained in all directions, so differences in recording angles can affect the reflection value received (Jensen, 2013).

Based on this, the study applies topographic correction. However, as seen from the results of the classification of the distribution pattern of the detected changes, it tends to have a similar pattern to the topographic relief in the research area.

This is influenced by the unsuccessful topographic correction process on the image which causes differences in topographic conditions to be considered as a change. The unsuccessful topographic correction causes the same object to have different intensity values, causing misclassification in the clustering process. (Fang et al., 2020; Li et al., 2015; Umarhadi & Danoedoro, 2019). Correct neither does topography capable overcome different corner recordings on both image.

**Table 2.** Class Change Area Distribution List

Class	No Change		Degradation		Devegetation		Avegetation	
	(Ha)	(%)	(Ha)	(%)	(Ha)	(%)	(Ha)	(%)
K_HS	1050.23	41.25	474.51	18.64	233.79	9.18	711.00	27.93
K_S2	<b>1224.07</b>	<b>48.08</b>	361.25	14,19	410.96	16,14	558.82	21.95
K_RE	789.29	31.00	<b>702.19</b>	<b>27.58</b>	492.67	19.35	468.85	18.42

Class	No Change		Degradation		Devegetation		Avegetation	
K_HSS2	1044.48	41.03	223.10	8.76	479.90	18.85	<b>729.25</b>	<b>28.64</b>
K_HSRE	1035.13	40.66	250.24	9.83	<b>502.91</b>	<b>19.75</b>	671.18	26.36
K_S2RE	847.99	33,31	641.97	25.22	419.05	16.46	617.16	24.24
K_HSS2RE	1016.97	39.95	254.11	9.98	491.23	19.30	729.16	28.64

Source: Research Results, 2021

Figure 3. Distribution Pattern K-means classification

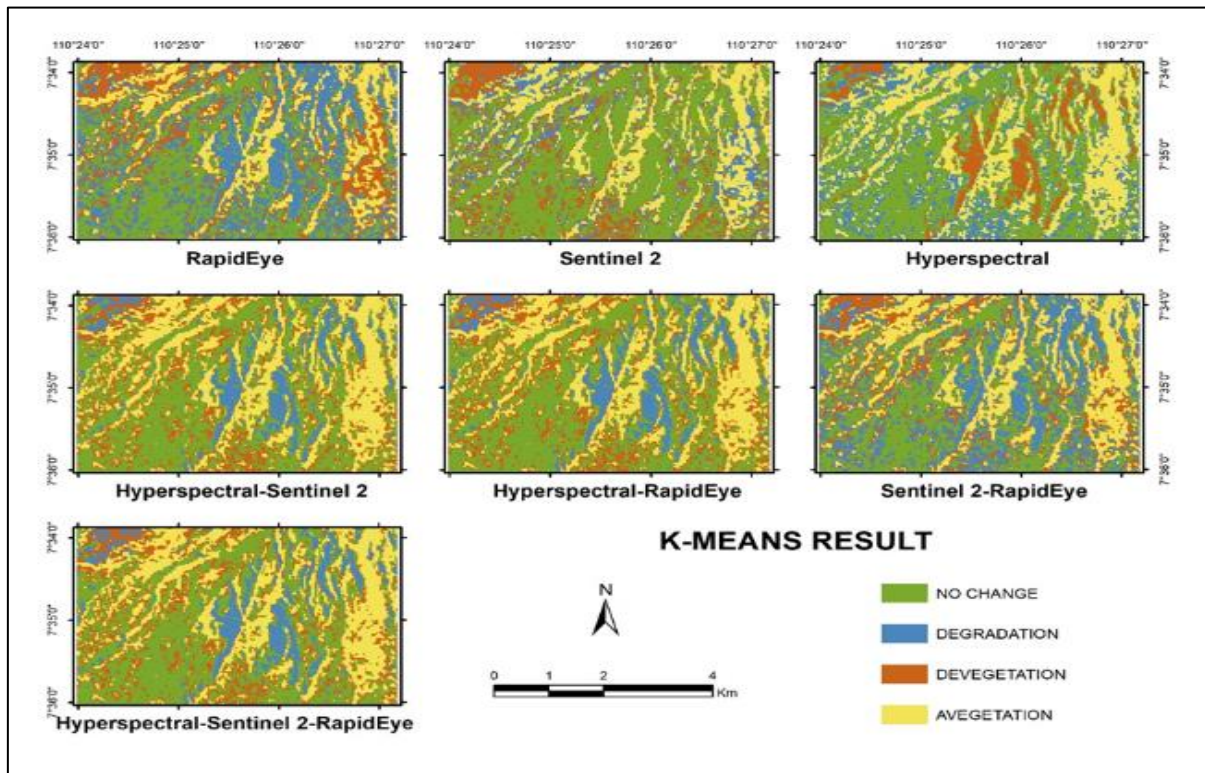


Table 3. Accuracy Results in Each Image Level

Imagery Datasets	Accuracy (%)
Hyperspectral	32.50
Sentinel 2A Simulation	31.50
Simulation Rapideye	<b>33.50</b>
Hyperspectral - Sentinel 2a Simulation	31.00
Hyperspectral - Simulation Rapideye	31.50
Simulation 2a - Simulation Rapideye	33.00
Hyperspectral - Sentinel Simulation 2a - Simulation Rapideye	31.00

Source: Research Results, 2021

### 3. Discussion

Based on the research and results analysis, there are several findings. In the analysis of vegetation change detection to prove the ability of a method and/or data, it

is necessary to select a research area that has high changes or is following the desired change objectives. In this study, the research area, part of which is a National Park Area,

has a low level of change so the identification of changes is difficult to do.

The temporal image dataset used needs to be considered carefully. The use of multisensory data will be a separate obstacle that will require careful consideration of geometric precision, radiometric values, gray levels, and image recording angles. Geometric precision in change detection analysis is very important because it will affect the results. The results can be overestimated due to pixel shifts which are considered to be changes. Radiometric and image gray levels play a role in spectral object recognition where this will be an obstacle that will arise due to the influence of sensor differences, vegetation phenology effects, and others, so adjustments are needed with the radiometric normalization method.

The difference in image recording angles is a difficult obstacle to overcome because it will affect the shadow effect, especially in areas with dynamic topography. The effect of this causes differences in values in pixels that have the same object but are in different positions. These differences in value can be compensated by applying a topographic correction method. However, it is necessary to select the best method according to the conditions in the research area and the dataset owned. Because no matter how good the correction method is, it will depend heavily on the data and conditions of the research area.

This study also found that differences in spectral levels do not have much effect on detecting vegetation changes. This can happen because the spectral level data is compiled from the same database so that the recognition of vegetation objects is not much

different. In addition, there is an anomaly where the image level that has a limited band has better accuracy. It can be seen that the highest accuracy can be achieved by the RapidEye simulation image level and at the combination level if there is a combination, with RapidEye the accuracy will increase. This anomaly needs to be studied further regarding its effect, whether it is caused by the number of spectral channels increasing noise or the presence of a channel composition that can recognize vegetation changes better.

## CONCLUSION

Mapping of vegetation changes using multi-sensor hyperspectral data by stacking spectral levels and the K-means CVA method was successfully applied, but the accuracy was low. The distribution pattern of vegetation changes mapped at each image level was similar. The highest accuracy achieved was 33.5% by the RapidEye simulation image level. Although the correction method has been applied to improve data quality, the method has not been able to improve data quality that has become poor due to differences in image acquisition angles. Therefore, the use of multi-sensor data is not recommended in detecting changes. The selection of correction methods, especially topographic correction, is very important if the research area is in a dynamic topography. Based on the accuracy value, it is also known that the difference in spectral levels does not have much effect on detecting vegetation changes, as evidenced by the difference in accuracy of each spectral level and its combination which is only around 0.5% - 2.5%. With the involvement of the community in this program, the greater the

number of participants involved in the mapping process, the stronger the results of decisions and policies determined by the community and village government (Ayuningtyas, 2022).

### THANK YOU NOTE

The author would like to thank the research funding provided through the 2021 Final Project Recognition Program by Gadjah Mada University. The PRISMA data used in this study were provided by the Italian Space Agency (ASI), and © Italian Space Agency (ASI), and delivered under the ASI License for use.

### REFERENCE

- Ayuningtyas, E. A. (2022). Pemetaan Partisipatif untuk Bahaya Longsor dan Jalur Evakuasi di Desa Hargomulyo, Kabupaten Kulonprogo, DIY. *Jurnal Geografika (Geografi Lingkungan Lahan Basah)*, 3(2), 78-91.
- Cavalli, R. M. (2023). The Weight of Hyperion and PRISMA Hyperspectral Sensor Characteristics on Image Capability to Retrieve Urban Surface Materials in the City of Venice. *Sensors*, 23 (1). <https://doi.org/10.3390/s23010454>
- Celik, T. (2009). Unsupervised change detection in satellite images using principal component analysis and  $\kappa$ -means clustering. *IEEE Geoscience and Remote Sensing Letters*, 6 (4), 772–776. <https://doi.org/10.1109/LGRS.2009.2025059>
- Chughtai, A.H., Abbasi, H., & Karas, I.R. (2021). A review on change detection method and accuracy assessment for land use land cover. *Remote Sensing Applications: Society and Environment*, 22 (March), 100482. <https://doi.org/10.1016/j.rsase.2021.100482>
- Chunhui, Z., Bing, G., Lejun, Z., & Xiaoqing, W. (2018). Classification of Hyperspectral Imagery based on spectral gradient, SVM ,and spatial random forest. *Infrared Physics and Technology*, 95 (January), 61–69. <https://doi.org/10.1016/j.infrared.2018.10.012>
- El Abbassi, M., Overbeck, J., Braun, O., Calame, M., van der Zant, HSJ, & Perrin, M.L. (2021). Benchmark and application of unsupervised classification approaches for univariate data. *Communications Physics*, 4 (1), 1–9. <https://doi.org/10.1038/s42005-021-00549-9>
- Fang, L., He, N., Li, S., Plaza, A. J., & Plaza, J. (2018). A New Spatial-Spectral Feature Extraction Method for Hyperspectral Images Using Local Covariance Matrix Representation. *IEEE Transactions on Geoscience and Remote Sensing*, 56 (6), 3534–3546. <https://doi.org/10.1109/TGRS.2018.2801387>
- Fang, Y., Zhao, J., Liu, L., & Wang, J. (2020). Comparison of eight topographic correction algorithms applied to Landsat-8 oil imagery based on the dem. *IOP Conference Series: Earth and Environmental Science*, 428 (1). <https://doi.org/10.1088/1755-1315/428/1/012051>
- Ghamisi, P., Plaza, J., Chen, Y., Li, J., & Plaza, A. J. (2017). Advanced Spectral Classifiers for Hyperspectral Images: A review. *IEEE Geoscience and Remote Sensing Magazine*, 5 (1), 8–32. <https://doi.org/10.1109/MGRS.2016.2616418>
- Ghamisi, P., Yokoya, N., Li, J., Liao, W., Liu, S., Plaza, J., Rasti, B., & Plaza, A. (2017). Advances in Hyperspectral Image and Signal Processing: A

- Comprehensive Overview of the State of the Art. In *IEEE Geoscience and Remote Sensing Magazine* (Vol. 5, Issue 4, pp. 37–78). <https://doi.org/10.1109/MGRS.2017.2762087>
- Ghosh, S., Patra, S., & Ghosh, A. (2009). An unsupervised context-sensitive change detection technique based on modified self-organizing feature map neural network. *International Journal of Approximate Reasoning*, 50 (1), 37–50. <https://doi.org/10.1016/j.ijar.2008.01.008>
- González-González, A., Villegas, J.C., Clerici, N., & Salazar, J.F. (2021). Spatial-temporal dynamics of deforestation and its drivers indicate the need for locally adapted environmental governance in Colombia. *Ecological Indicators*, 126. <https://doi.org/10.1016/j.ecolind.2021.107695>
- Hasanlau, M., & Seydi, ST (2018). Sensitivity analysis on the performance of different unsupervised threshold selection methods in hyperspectral change detection. *2018 10th IAPR Workshop on Pattern Recognition in Remote Sensing, PRRS 2018*, 6–9. <https://doi.org/10.1109/PRRS.2018.8486355>
- Jensen, J.R. (2013a). *Remote Sensing of the Environment: An Earth Resource Perspective: Pearson New International Edition*. Pearson Education. <https://books.google.co.id/books?id=fhGpBwAAQBAJ>
- Jensen, J.R. (2013b). *Remote Sensing of the Environment: An Earth Resource Perspective: Pearson New International Edition*. Pearson Education.
- Khan, M.J., Khan, H.S., Yousaf, A., Khurshid, K., & Abbas, A. (2018). Modern Trends in Hyperspectral Image Analysis: A Review. *IEEE Access*, 6 (June), 14118–14129. <https://doi.org/10.1109/ACCESS.2018.2812999>
- Kuzera, K., Rogan, J., & Eastman, J.R. (nd). *Monitoring Vegetation Regeneration and Deforestation Using Change Vector Analysis: Mt. St. Helens Study Area*.
- Lehnert, L.W., Meyer, H., Obermeier, W.A., Silva, B., Regeling, B., & Bendix, J. (2018). *Hyperspectral Data Analysis in R: the hsdar Package*. <https://doi.org/10.18637/jss.v089.i12>
- Leutner, B., Horning, N., Schwalb-Willmann, J., Hijmans, R.J., & Maintainer, J. (2019). *Package “RStoolbox” Title Tools for Remote Sensing Data Analysis*.
- Li, H., Xu, L., Zhang, Z., Shen, H., Li, W., & Cao, L. (2015). A land cover adaptive topographic correction and evaluation method for remote sensing data. *International Geoscience and Remote Sensing Symposium (IGARSS), 2015-Novem* (1), 3850–3853. <https://doi.org/10.1109/IGARSS.2015.7326664>
- Lillesand, T., Kiefer, R. W., & Chipman, J. (2015a). *Remote Sensing and Image Interpretation, 7th Edition*. Wiley.
- Lillesand, T., Kiefer, R. W., & Chipman, J. (2015b). *Remote Sensing and Image Interpretation, 7th Edition*. Wiley. <https://books.google.co.id/books?id=eQXYBgAAQBAJ>
- Liu, S. (2015). *Sequential Spectral Change Vector Analysis for Iteratively Discovering and Detecting Multiple Changes in Hyperspectral Images. March*. <https://doi.org/10.1109/TGRS.2015.2396686>

- Liu, S., Bruzzone, L., Bovolo, F., & Du, P. (2012). Unsupervised hierarchical spectral analysis for change detection in hyperspectral images. *Workshop on Hyperspectral Image and Signal Processing, Evolution in Remote Sensing*, June. <https://doi.org/10.1109/WHISPERS.2012.6874245>
- Lu, D., Li, G., & Moran, E. (2014). Current situation and need for change detection techniques. *International Journal of Image and Data Fusion*, 5 (1), 13–38. <https://doi.org/10.1080/19479832.2013.868372>
- Lu, D., Mausel, P., Brondízio, E., & Moran, E. (2004). Change detection techniques. *International Journal of Remote Sensing*, 25 (12), 2365–2401. <https://doi.org/10.1080/0143116031000139863>
- Seydi, ST, & Hasanlou, M. (2017). A new land-cover match-based change detection for hyperspectral imagery. *European Journal of Remote Sensing*, 50 (1), 517–533. <https://doi.org/10.1080/22797254.2017.1367963>
- Sinaga, KP, & Yang, MS (2020). Unsupervised K-means clustering algorithm. *IEEE Access*, 8, 80716–80727. <https://doi.org/10.1109/ACCESS.2020.2988796>
- Sun, L., Zhao, D., Zhang, G., Wu, X., Yang, Y., & Wang, Z. (2022). Using SPOT VEGETATION for analyzing dynamic changes and influencing factors on vegetation restoration in the Three-River Headwaters Region in the last 20 years (2000–2019), China. *Ecological Engineering*, 183 (July), 106742. <https://doi.org/10.1016/j.ecoleng.2022.106742>
- Tripathi, M. K., Govil, H., & Diwan, P. (2019). Petrography, XRD analysis, and identification of talc minerals near Chhabadiya village of Jahajpur region, Bhilwara, India through Hyperion hyperspectral remote sensing data. *2019 2nd International Conference on Intelligent Communication and Computational Techniques, ICCT 2019*, 75–78. <https://doi.org/10.1109/ICCT46177.2019.8969008>
- Umarhadi, DA, & Danoedoro, P. (2019). Correcting topographic effect on Landsat-8 images: an evaluation of using different DEMs in Indonesia. *November 2019*, 41. <https://doi.org/10.1117/12.2549109>
- Visual Information Solutions, I. (1988). *FLAASH Module User's Guide 20FLA43DOC*. <http://www.csie.ntu.edu.tw/~cjlin/libsvm>
- Wu, J. (2012). *K-means Based Consensus Clustering*. Springer Science & Business Media. [https://doi.org/10.1007/978-3-642-29807-3\\_7](https://doi.org/10.1007/978-3-642-29807-3_7)
- Zheng, Z., Wan, Y., Zhang, Y., Xiang, S., Peng, D., & Zhang, B. (2021). ISPRS Journal of Photogrammetry and Remote Sensing CLNet: Cross-layer convolutional neural network for change detection in optical remote sensing imagery. *ISPRS Journal of Photogrammetry and Remote Sensing*, 175 (March), 247–267. <https://doi.org/10.1016/j.isprsjprs.2021.03.005>